# Benthic foraminiferal species tolerance for hydrothermal activity: a case of study from the Lucky Strike vent field.

Pierre-Antoine Dessandier[1], Giuliana Panieri[2], Riwan Leroux[1], Ewan Pelleter[3], Sandra Fuchs[1], Alizé Bouriat[1], Audrey Boissier[3], Sandrine Cheron[3], Jozée Sarrazin[1]

1 Univ Brest, Ifremer, BEEP, F-29280 Plouzané, France

2 Department of Geosciences, UiT - The Arctic University of Norway, 9037, Tromsø, Norway

3 Geo-Ocean, University Brest, CNRS, Ifremer, UMR6538, Plouzane, France

Corresponding author: Pierre-Antoine Dessandier, pierre.antoine.dessandier@ifremer.fr

## Abstract

Hydrothermal vent fields represent dynamic environments hosting rich ecosystems. At the Mid-Atlantic Ridge, the Lucky Strike (LS) vent field has been the focus of multiple biological studies. While ecological studies have been focusing on microbial and macrofaunal communities, some groups still remained out of the scope. We present here the first ecological study of benthic foraminifera inhabiting soft sediments in the peripheries of hydrothermal edifices at LS. A total of fifteen blade cores were analyzed. We combine microhabitat environmental descriptors with faunal density and diversity of benthic foraminifera (living & fossil) to investigate the impact of hydrothermal activity on their ecology. The far periphery, ~150 m away from vents, harbors a community of diverse foraminifera feeding on pre-degraded organic matter characterized by a phytoplankton detrital signal, as shown by the isotopic signal of the organic matter. Communities located at intermediate distance (~ 50 m) from venting showed the presence of opportunistic species likely feeding on chemosynthetic

microorganisms. Finally, environments closer to active sites (few meters) showed very low abundance of living individuals, as the presence of harsh environmental conditions may limit foraminiferal growth. Unexpectedly, the presence of widespread iron-oxidizer bacterial biofilms was associated to the dissolution of all biogenic carbonate content raising questions on their impact on regional carbon budget.

Key words: Benthic foraminifera, hydrothermal activity, Lucky Strike vent field, microbial biofilm.

## 1. Introduction

Benthic foraminifera are marine micro-organisms that represent more than 50% of the eukaryotic biomass in many deep-sea habitats and influence the structure and dynamics of marine biological communities, with larger benthic organisms from the meiofauna and macrofauna as predators and microorganisms as preys (Gooday et al., 1994). Benthic foraminifera have been widely studied as fossils in marine systems for more than a century and as living individuals for ecological purpose since the 1960s'. However, very few studies have been conducted on benthic foraminifera from deep-sea hydrothermal vents (Molina-Cruz and Ayala-Lopez, 1988; Jonasson et al., 1995; Burkett et al., 2018; Krüger et al., 2025) because of complex sampling techniques (hard substrates, use of submersible) and the usual focus on microbes and macrofauna in these environments.

Benthic foraminiferal distribution in the marine sediment is mainly controlled by the spatially opposed contents of organic matter and oxygen (Jorissen et al., 1995; Mackensen et al., 1995), but also by organic matter quality and source (e.g., Altenbach et al., 1999; Loubere and Fariduddin, 1999; Dessandier et al., 2016). In deep-sea environments, the food source for benthic foraminifera is often limited to degraded detrital and microbial organic matter (Alongi

48 and Pichon, 1988; Gooday et al., 1992, Gooday et al., 2008). In extreme environments, where
49 fluids enhance microbial activities, benthic foraminifera can thrive feeding on certain groups of
50 bacteria, where the conditions allow them to survive (Panieri, 2006; Bernhard and Panieri,
51 2018; Dessandier et al., 2019).

52 Extreme environments with fluids-rich sediments may offer a nutrient-rich microbial food
53 source for benthic foraminifera, yet they also represent a potentially harsh environment due to
54 their challenging physical and chemical conditions (e.g., Kurt and Barry, 1998; Dessandier et
55 al., 2019). Hydrothermal vents are dynamic systems where cold seawater penetrate through
56 cracks in the ocean crust and is heated and enriched in dissolved metals and sulfur in contact
57 with rocks overlying the magma chamber. This process results in the emergence of hot, slightly
58 acidic and chemically reduced fluids. Most of the metals dissolved in the ascending vent fluids
59 precipitate when they mix with the surrounding cold seawater, resulting in black- and white
60 smoker chimneys, large sulfide edifices and later, extensive mounds of accumulated massive
61 sulfide. Hydrothermal vent fields are commonly referred as to “oases of life”, harboring
62 luxuriant chemosynthetic faunal communities (Fisher et al., 2007). Associated food webs are
63 mainly based on local microbial chemosynthesis (Childress and Fisher, 1992), performed by
64 free-living and symbiotic chemoautotrophic microorganisms that utilize the chemical energy
65 released by the oxidation of reduced chemicals species ($H_2$, $H_2S$, $CH_4$, Fe) present in the
66 hydrothermal fluids (Childress and Fisher, 1992, Schmidt et al. 2008). In Juan de Fuca Ridge
67 (North Pacific Ocean), the distribution of foraminifera was shown to be influenced by
68 temperature, pH and substratum types, resulting in their absence at temperature higher than
69 20°C and on unstable surfaces such as friable anhydrite which prevents the attachment of
70 agglutinated species (Jonasson et al., 1995). Among hydrothermal vent systems, the Lucky
71 Strike vent field has been one of the most studied ecosystems since its discovery in 1992 and
72 with more than 15 years of continuous multidisciplinary observations through the EMSO-

Azores observatory deployed in 2010 (Matabos et al., 2025). Over these studies, it has been pointed out that regional distributions of macro- and meiofauna depend on abiotic parameters such as pH, temperature, sulfides and metals (e.g., Sarrazin et al., 2015, see Matabos et al., 2025 for a review). However, no studies yet filled the gaps about the role of the benthic foraminifera in this system. Given its numerous active vent sites and well documented biotic and abiotic conditions, the Lucky Strike vent field provides an ideal setting for investigating benthic foraminiferal ecology in hydrothermal ecosystems and their role in influencing regional biodiversity. This study presents the first analysis of benthic foraminifera from the Lucky Strike vent field, integrating living and fossil foraminiferal individuals and environmental conditions across gradients of hydrothermal influence and associated microbial biofilms.

## 2. Study area

The Lucky Strike hydrothermal vent field on the Mid-Atlantic Ridge (MAR) at 37°17'N is one of the largest fields. It is located at ~1,700 m water depth and its ~25 active edifices are surrounding a 200 m diameter lava lake (Ondréas et al., 2009). Biological and geological evidence indicate a long venting history at Lucky Strike, with recent lava footprint analyses suggesting that modern volcanic activity has driven the resurgence of hydrothermal venting (Langmuir et al., 1997). Several active and inactive edifices have been identified since the first exploration of the field in 1993 (Fouquet et al., 1995). In addition to the sulfide structures, the seafloor is characterized by sulfide deposits and covered by hydrothermal breccia of basaltic glass and plagioclase crystals indurated by silica and barite (Langmuir et al., 1997). The sediments surrounding the structures contain high concentration of metals such as Fe, Cu and Zn, particularly enriched at the Capelinhos vent site where the fault configuration enables hot fluid outflow (>300°C) (Fig. 1, Cotte et al., 2020).

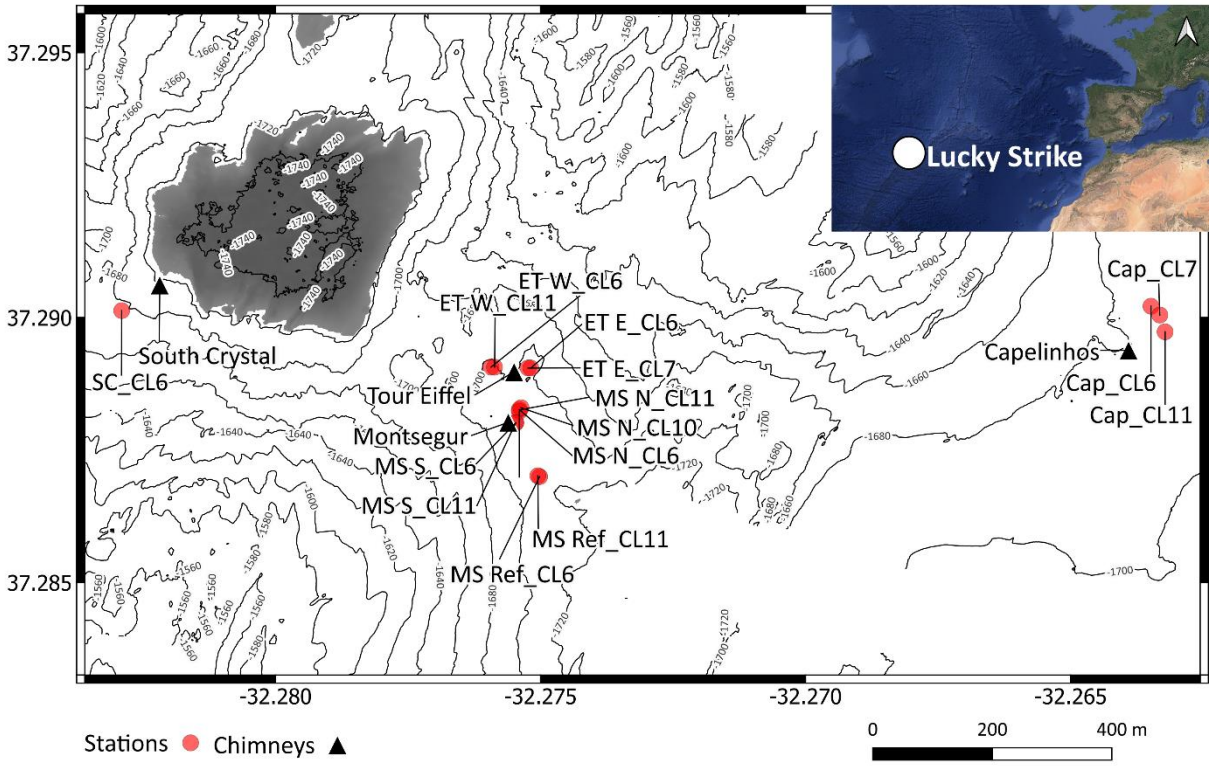


Fig. 1. Location of the Lucky Strike vent field on the Mid-Atlantic Ridge (inset) and of the sediment cores (grey circles) collected in 2020 near four active hydrothermal edifices (black triangle).

As observed in many different hydrothermal fields, the metabolic activity is greatly enhanced by symbiosis with chemosynthetic microorganisms. That results at Lucky Strike in a strong dominance of *Bathymodiolus azoricus* mussel assemblages (Van Dover, 1995; Desbruyeres et al., 2001) that create habitats hosting at least 79 associated species, each occupying distinct ecological niches (Sarrazin et al., 2015; Husson et al., 2017; Sarrazin et al., 2020). Two other assemblages, dominated respectively by *Mirocaris fortunata* shrimp and by *Peltospira smaragdina* gastropods, dominate warmer areas (Sarrazin et al., 2022). The geochemistry of the plumes showed a strong dilution of the fluid a few meters (5 to 10 m) away from the venting locations, as suggested by measurements of temperature and pH gradients near one of the largest and most studied edifices (i.e., Eiffel Tower; Sarradin et al., 2009). The area of exported

particles does not reach 500 m and the influence of the vent field on the open ocean remains restricted (Khripounoff et al., 2000). Even though the Lucky Strike vent field differs from the other Mid-Atlantic Ridge vent sites by the absence of well-developed peripheral macrofauna (Van Dover et al., 1996), the vent primary chemosynthetic production is exported at least as far as ~90 m in the field (Alfaro-Lucas et al., 2020). The peripheral fauna harbors unique species and functional entities that contribute to increase the biodiversity at the vent field scale (Alfaro-Lucas et al., 2020).

## 3. Material and methods

During the MoMARSAT cruise in September 2020, 15 sediment blade cores have been collected using the remotely operated vehicle *Victor6000* (Ifremer, Fig.1). Among them, 1 core was not analyzed due to missing sedimentary material, and 3 of them targeted microbial mats, visually attributed to iron-oxidizers biofilms, most likely zetaproteobacteria (Astorch-Cardona et al., 2023). Various venting locations were targeted (i.e., near Eiffel Tower, Montsegur, Capelinhos and South Crystal edifices) in addition to a more distal location ~100 m away from active venting (called Montsegur-Ref, Fig. 1). Each core has been sliced on board every centimeter and split in two equivalent volumes for each horizon, one preserved at -20°C for geochemical analyses and one preserved in a solution of Rose Bengal 2 g $L^{-1}$ in 96% ethanol during several weeks for living benthic foraminiferal identification, individually wet-picked in petri dishes (Table 1). Then, the samples were wet sieved under filtered (0.2 µm) seawater and all foraminiferal analyses were done on the >63 µm size fraction. Since the preservation used was not the best for soft-walled foraminifera as formalin would have been, this study may underestimate this group. However, a previous check of formalin-preserved samples without staining did not show high abundance of soft-walled foraminifera in the area and in order to be consistent with comparable literature in vent studies focuses on benthic foraminifera, ethanol

preservation has been used. All living individuals (>63 µm) were sorted for foraminiferal counts. Dead individuals (>63 µm) were sorted after drying the samples and using an Otto microsplitter to estimate the foraminiferal densities. The taxonomy of benthic foraminiferal species has been realized thanks to the Atlas of Benthic Foraminifera (Holbourn et al., 2013) and Loeblich and Tappan (1987). Specimens were considered living when all chambers, except the last one, were stained. In case of doubt, notably for the miliolids, tests were broken to ensure that the staining came from internal cytoplasm.

Table 1. List of collected samples. Note that Cap_CL11 was analyzed for geochemistry only and Cap_CL6 for foraminifera only. Geoch. and Foram. correspond to the horizons analyzed for geochemical and foraminiferal data, respectively. S = Specific richness, H' = Shannon index, E = Evenness index.

| Core name | Site | Station code | Day | Lat. N | Long. W | Water depth (m) | Geoch. | Foram. | Indiv. | S | H' | E |
|---|---|---|---|---|---|---|---|---|---|---|---|---|
| 755-3_CL6 | Montsegur N | MS N_CL6 | 15.09.2020 | 37°17.296' | 32°16.524' | 1703 | 0-5 cm | 0-1 cm | 16 | 8 | 1,808 | 0,7623 |
| 755-3_CL10 | Montsegur N | MS N_CL10 | 15.09.2020 | 37°17.294' | 32°16.524' | 1703 | 0-8 cm | 0-5 cm | 33 | 14 | 2,317 | 0,7249 |
| 755-3_CL11 | Montsegur N | MS N_CL11 | 15.09.2020 | 37°17.298' | 32°16.522' | 1703 | 0-6 cm | 0-5 cm | 34 | 7 | 1,582 | 0,695 |
| 757-5_CL6 | Capelinhos | Cap_CL6 | 17.09.2020 | 37°17.413' | 32°15.809' | 1684 | NA | 0-1 cm | 1 | 1 | 0 | 1 |
| 757-5_CL11 | Capelinhos | Cap_CL11 | 17.09.2020 | 37°17.384' | 32°15.793' | 1684 | 0-6 cm | NA | NA | NA | NA | NA |
| 757-5_CL7 | Capelinhos | Cap_CL7 | 17.09.2020 | 37°17.403' | 32°15.799' | 1684 | 5-7 cm | 0-5 cm | 3 | 2 | 0,6365 | 0,9449 |
| 759-7_CL11 | Eiffel Tower W | ET W_CL11 | 21.09.2020 | 37°17.344' | 32°16.556' | 1697 | 0-5 cm | 0-5 cm | NA | NA | NA | NA |
| 759-7_CL6 | Eiffel Tower W | ET W_CL6 | 21.09.2020 | 37°17.344' | 32°16.552' | 1697 | 0-5 cm | 0-5 cm | 81 | 20 | 2,525 | 0,6245 |
| 760-8_CL7 | Eiffel Tower E | ET E_CL7 | 22.09.2020 | 37°17.343' | 32°16.514' | 1701 | 0-7 cm | 0-5 cm | 7 | 5 | 1,475 | 0,8743 |
| 760-8_CL6 | Eiffel Tower E | ET E_CL6 | 22.09.2020 | 37°17.343' | 32°16.511' | 1701 | 0-5 cm | 0-5 cm | 83 | 14 | 2,205 | 0,6476 |
| 761-9_CL6 | South Crystal | SC_CL6 | 22.09.2020 | 37°17.408' | 32°16.974' | 1719 | 0-9 cm | 0-5 cm | 38 | 11 | 2,025 | 0,6886 |
| 762-10_CL6 | Montsegur | MS_CL6 | 24.09.2020 | 37°17.281' | 32°16.528' | 1702 | 0-4 cm | 0-4 cm | 1 | 1 | 0 | 1 |
| 762-10_CL11 | Montsegur | MS_CL11 | 24.09.2020 | 37°17.281' | 32°16.528' | 1702 | 0-4 cm | 0-4 cm | NA | NA | NA | NA |
| 763-11_CL11 | Montsegur Ref | MS Ref_CL11 | 24.09.2020 | 37°17.220' | 32°16.501' | 1712 | 0-8 cm | 0-5 cm | 58 | 16 | 2,497 | 0,7592 |
| 763-11_CL6 | Montsegur Ref | MS Ref_CL6 | 24.09.2020 | 37°17.221' | 32°16.503' | 1712 | 0-8 cm | 0-5 cm | 101 | 22 | 2,333 | 0,4684 |

Bulk chemical composition of each surface sediment (0-1 cm) sample was determined using a wavelength dispersive X-ray fluorescence spectrometer (BRUCKER AXS S8 Tiger) at Ifremer. Samples were freeze-dried and ground to a powder (90% of particles < 80 µm) using an agate pestle and mortar. Major elements and selected trace elements were analyzed on pressed pellets

and fused beads (with a specific preparation for S analysis of sulfide-rich sediment; supplementary 1). After acquisition, the measured net peak intensities, corrected for inter-element effects, were converted into concentrations using calibration curves generated from analysis of certified geochemical standard powders (measured under identical analytical conditions).

Total organic carbon and its isotopic signature (TOC, $\delta^{13}C_{TOC}$) have been measured using a LECO TruMac, after carbonate dissolution (HCl 1N) at Ifremer. Accelerator Mass Spectrometry $^{14}C$ dating has been performed on 7 samples from two blade cores, in order to estimate sedimentation rates near the active Eiffel Tower edifice (ET E_CL7) and at the periphery of the vent field (MS Ref_CL6). Radiocarbon dating was carried out at the Beta Analytic Radiocarbon Dating facilities in Miami, US. The age was converted into calendar years using the calibration program Calib 7.1 (Stuiver et al., 2014) with a marine reservoir age of -400 years that was incorporated within the Marine13 calibration curve (Reimer et al., 2013). Grain size was determined using a Mastersizer 3000 at Ifremer. The mode was used to characterize the habitat grain size after checking that all spectra were unimodal.

Faunal and environmental statistics have been performed using the software Primer v6.0 (Clarke and Warwick, 1994), for diversity indices (specific richness, Shannon and Evenness indices), principal component analysis (PCA) and matrices calculations (BioEnv). A PCA has been performed including standardized (minus average, divided by standard deviation) environmental parameters ($Fe_2O_3$, S, Cu, Ba, MnO, $SiO_2$, CaO, TC, TOC, $\delta^{13}C$ and grain size) and standardized living faunal descriptors (individuals, specific richness and Shannon Index values) in order to investigate the control factors of the faunal distribution. A redundancy analysis (RDA) was performed to investigate the influence of environmental variables on the distribution of dead and living most abundant taxa in the 0-1 cm layer. Dead and living organisms were pooled together in order to restrain taphonomical impacts, such as seasonal

effects and to ensure robust interpretations as rarefaction curves tend to show underestimation through living fauna (supplementary 2). Six species and two taxonomic groups were kept for the RDA analysis: *Quinqueloculina auberiana*, *Lobatula wuellerstorfi*, *Cibicides pachyderma*, *Cruciloculina triangulis*, *Epistominella exigua*, *Gavelinopsis translucens*, pooled *Fissurina* species and pooled non calcareous species. We decided to pool species of *Fissurina* genus, even though a large proportion of them come from the same species (i.e., *F. orbignyana*), because very little is known about their ecology and all species were distributed in a similar way. However, we can't exclude that this approach is biased by the fact that some species of this genus may have a different ecology, hence *Fissurina* species are separated in the statistical approach. RDA was performed with the R software (R core team, 2025) and the vegan package (Oksanen et al., 2001). A forward selection was implemented to select the environmental variables significantly explaining the species distribution (function ordistep of the vegan package).

A correlation of environmental (Euclidean distance) and faunal (Bray-Curtis dissimilarity) matrices has been performed through the test BEST (BioEnv) to determine the main elements impacting the distribution of both fossil and living fauna on the study area (2 tests on total abundances). Environmental parameters considered in the calculation were grain size, $SiO_2$, $Fe_2O_3$, MnO, CaO, S, Ba, Cu, $\delta^{13}C_{TOC}$, TOC and TC.

## 4. Results

### 4.1. Habitat characterization

Sediment microhabitats have been studied through their particulate element composition, the main elements measured in each core surface (0-1 cm) have been represented as bar charts of relative abundance (Fig. 2) and secondary elements as superposed curves.

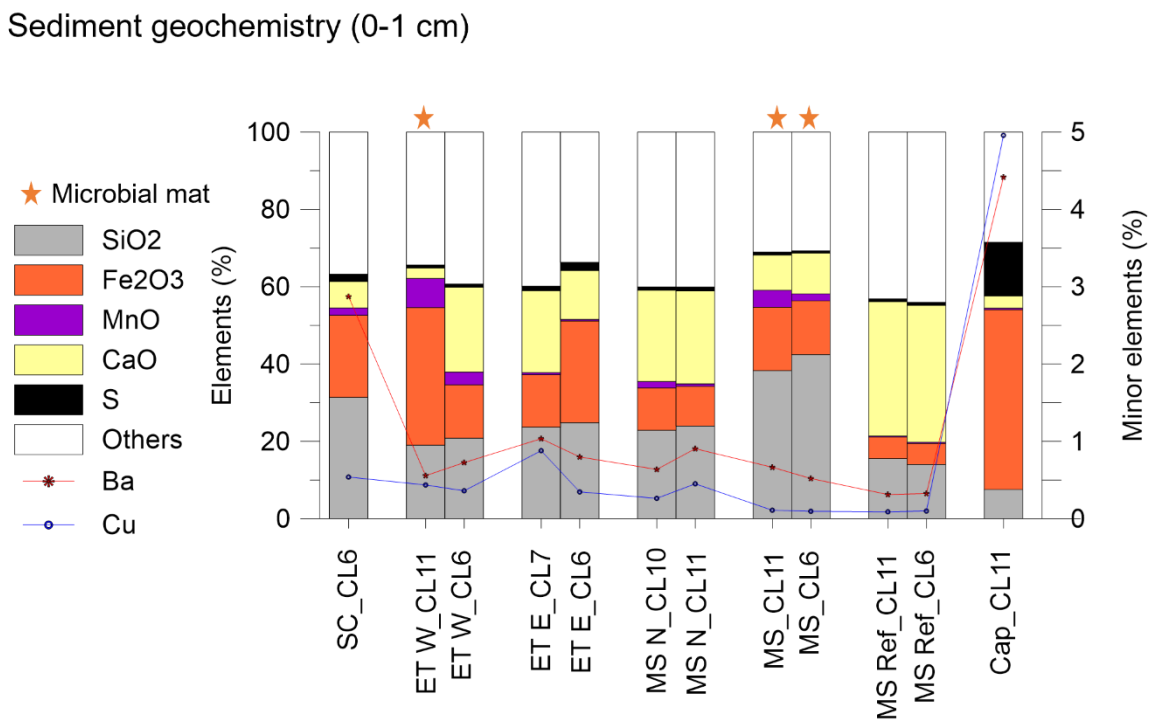


202

203 Fig. 2. XRF analyses of top layers (0-1 cm) of the 12 sediment cores sampled in 2020 on the
204 Lucky Strike vent field (Mid-Atlantic Ridge). Ba and Cu are plotted as minor elements (right
205 scale).

206

207 CaO represented the main component of stations MS N and MS Ref ranging from 24 to 35%.
208 $SiO_2$ values ranged from 8% (station Cap_CL6) to 42% (station MS_CL6). $Fe_2O_3$ and S were
209 the most abundant elements in station Cap_CL6, reaching 46% and 14%, respectively. This
210 station also showed peaks of Ba (4.4%) and Cu (4.9%). $Fe_2O_3$ (36%) and MnO (8%) were high
211 in station ET W_CL6. Finally, relatively high $Fe_2O_3$ (21%) and Ba (2.8%) have been measured
212 in station SC_CL6. Major elements signature of surface sediments is related to mixing of
213 particles form three different origin (Fig. 3): (1) pure pelagic sediments (carbonate), (2) pure
214 metalliferous sediments (sulfides and/or oxides) and (3) mafic rocks (i.e., basalt) from the
215 oceanic crust.

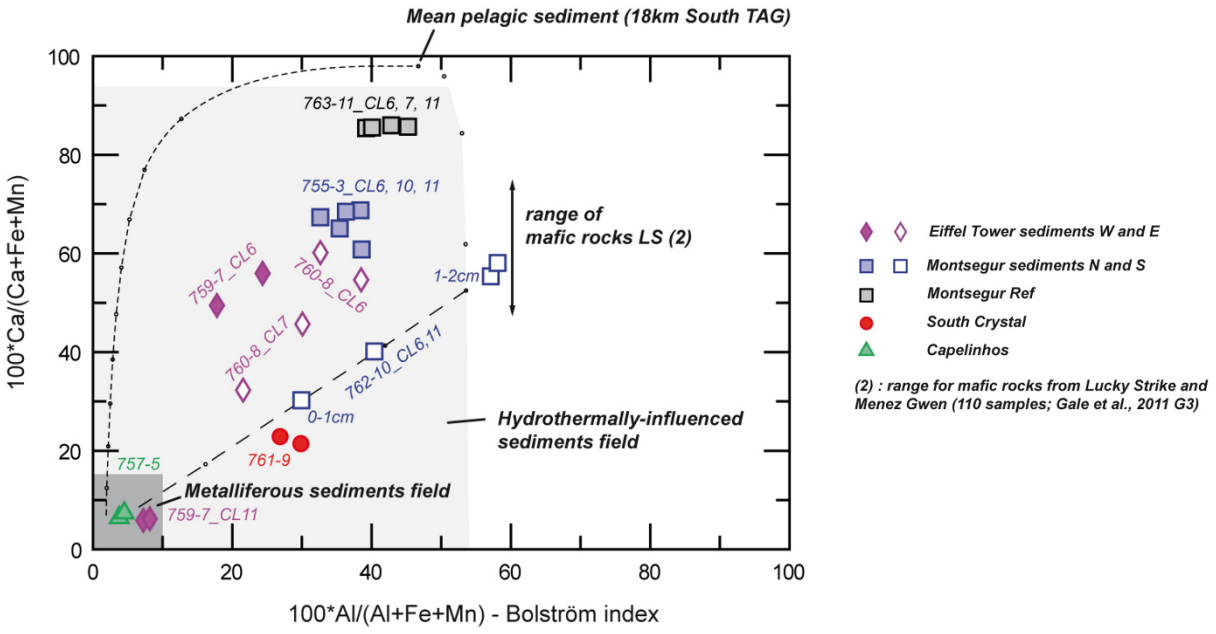


Fig. 3. Bolström diagram representing the geochemical analyses of the top sediment layers (0-1 cm) in the peripheries of four active edifices on the Lucky Strike vent field (Mid-Atlantic Ridge), corresponding to cores analyzed for foraminiferal analyses.

Sediments from Montsegur_Ref shows only little hydrothermal particles contribution and plot close to the mean pelagic sediment composition. Sediments from Capelinhos and two from Eiffel Tower W plot inside the metalliferous sediment field (Fig. 3) indicating a strong hydrothermal influence, with high dissolved metals content in pore water profiles (supplementary 3). Sediments from Montsegur S and South Crystal plot on a mixing line between metalliferous sediments and mafic rocks. Distribution of other sediments in Figure 3 indicate a variable mixture of pelagic sediments, mafic rocks fragments and metalliferous sediments.

Sedimentation rates have been calculated from two different sites (supplementary 4), one in the vicinity of the Eiffel Tower edifice (ET E_CL7) and one in the south periphery of Lucky Strike (MS Ref_CL6). These sedimentation rates showed relatively stable trends, especially for the station MS Ref_CL6, indicating a mean value of 2.3 cm.kyr$^{-1}$, classical for deep sea Atlantic

sediments (Levin and Gooday, 2003). At the basis of the Eiffel Tower edifice, the sedimentation rate was 4.3 cm.kyr$^{-1}$.

Inorganic and organic carbon as well as $\delta^{13}C$ of organic carbon have been measured on surface sediment samples (0-1 cm) and summarized in Table 2. Total carbon (TC) data showed maximal values in MS Ref stations, exceeding 7.5%. Minimum values (<1%) were obtained in the three cores targeting microbial mats (ET W_CL11, MS_CL6 and MS_CL11) and in the SC_CL6 core. Maximal total organic carbon (TOC) values were obtained in station MS N_CL11, Cap_CL6 and MS Ref. $\delta^{13}C_{TOC}$ ranged from -25.4‰ (ET W_CL11) to -22.3‰ (MS Ref_CL11).

Table 2. Organic and inorganic carbon data.

| Core | TC (%) | TOC (%) | TOC st. dev. | $\delta^{13}C_{TOC}$ | $\delta^{13}C_{TOC}$ st. dev. |
|---|---|---|---|---|---|
| MS N_CL6 | 2.19 | 0.17 | 0.002 | -23.40 | 0.01 |
| MS N_CL10 | 4.68 | 0.22 | 0.012 | -22.63 | 0.35 |
| MS N_CL11 | 4.90 | 0.32 | 0.033 | -23.13 | 0.11 |
| Cap_CL11 | 1.21 | 0.30 | 0.000 | -23.58 | 0.00 |
| ET W_CL11 | 0.80 | 0.18 | 0.012 | -25.35 | 0.91 |
| ET W_CL6 | 4.43 | 0.23 | 0.007 | -23.35 | 0.11 |
| ET E_CL7 | 1.99 | 0.19 | 0.010 | -25.34 | 0.46 |
| ET E_CL6 | 4.13 | 0.29 | 0.014 | -23.87 | 0.15 |
| SC_CL6 | 0.73 | 0.22 | 0.014 | -25.11 | 0.35 |
| MS_CL6 | 0.21 | 0.21 | 0.016 | -24.35 | 0.53 |
| MS_CL11 | 0.39 | 0.17 | 0.013 | -24.66 | 0.41 |
| MS Ref_CL11 | 7.66 | 0.26 | 0.004 | -22.30 | 0.10 |
| MS Ref_CL6 | 8.02 | 0.27 | 0.002 | -22.34 | 0.11 |

## 4.2. Foraminiferal distribution

In total, 54 species have been identified on the whole study area. Living individuals showed contrasted densities and diversities (Table 1) with the highest number of individuals (101) and specific richness (22) in station MS Ref_CL6 and a minimum of 1 individual in station Cap_CL6. Relatively high diversity characterized stations MS Ref_CL6 and ET E_CL6 with

Shannon indexes of 2.5. The rest of the stations displayed Shannon index values ranging from 0.6 to 2.3.

When focusing on the dead individuals, the relationship between the specific richness and the number of identified individuals showed similar trends for most of the stations and rarefaction curves indicated that more than 90% of the species are identified within the first 300 individuals of the total assemblages (supplementary 2). Stations ET E_CL6 and MS Ref_CL6 showed the highest diversity with 30 and 28 species for 300 individuals, respectively. A minimum of 13 species for 300 individuals was observed in MS N stations. Three cores revealed the absence (or only one individual) of benthic foraminifera (MS_CL6 and CL11 and ET W_CL11) where microbial mats have been targeted for the sampling.

A PCA was conducted to investigate the environmental factors influencing living benthic foraminiferal communities (Fig. 4).

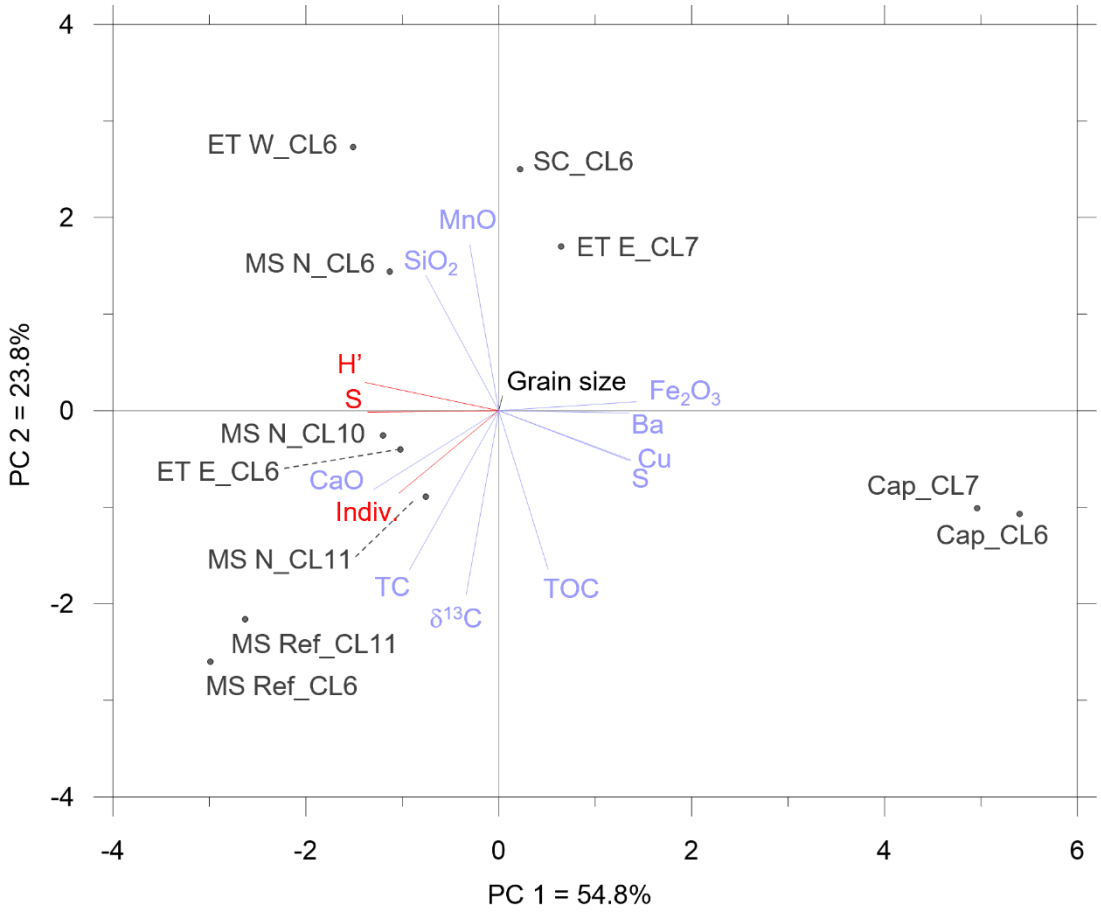

Fig. 4. Principal Component Analysis with environmental parameters in blue and biological metrics in red. H' = shannon index, S = specific richness, Indiv. = number of individuals.

The first two axes account for 78.6% of the total data variability, with PC1 explaining 54.8% and PC2 explaining 23.8% of the variance. PC1 seemed to correspond to hydrothermal inputs with positive loadings for the elements $Fe_2O_3$, S, Cu and Ba and slightly positive loading for TOC, while CaO displayed the most negative loading. Hence, the hydrothermal-derived elements on the PC1 particularly isolated the cores Cap_CL7 and Cap_CL6, representing the hydrothermal domain. SC_CL6 and ET E_CL7 also showed positive loading on PC1, suggesting a significant hydrothermal signal. The second axis suggested a control of the organic matter source with negative loadings of TC and $\delta^{13}C$ and CaO. Positive loadings on the PC2 were characterized by MnO and $SiO_2$. All cores showing negative loadings for both PC1 and PC2 were characterized by a pelagic sedimentation dominated by phytodetrital organic matter ($\delta^{13}C$ ~ -20 ‰ and high CaO content), representing the reference domain with cores MS Ref_CL11 and MS Ref_CL6. The last domain visible on the PCA was intermediate, showing a lower contribution of elements from the pelagic sedimentation (CaO) or from hydrothermal input ($Fe_2O_3$, S, Cu and Ba), resulting in higher contribution of $SiO_2$. MnO content suggested a slight influence of hydrothermal-derived particles, probably originating from low temperature Mn-oxides precipitation. The living foraminiferal signals plotted in the PCA demonstrate how fauna distributes on these environmental domains. The abundance of living benthic foraminifera was well correlated with the reference domain while faunal diversity better corresponded to the intermediate domain, suggesting an influence of the source of organic matter. BioEnv statistical tests (BEST, Primer v.06) was performed on both dead and living faunal communities with environmental data (Table 3). Both tests highlighted the control of $Fe_2O_3$ alone for the living communities and $Fe_2O_3$ with Ba for the dead ones as main control of

faunal variability (Table 3), confirming the impact of hydrothermal-derived microhabitats at a regional scale.

Table 3. Statistical test BioEnv (matrices correlation).

BioEnv (living fauna). significance: 4%

| Variables number | $R^2$ | Variables |
|---|---|---|
| 1 | 0.664 | $Fe_2O_3$ |
| 2 | 0.659 | $Fe_2O_3$. Ba |
| 2 | 0.652 | $Fe_2O_3$. Cu |
| 3 | 0.651 | $Fe_2O_3$. Ba. Cu |

BioEnv (dead fauna). significance: 2%

| Variables number | $R^2$ | Variables |
|---|---|---|
| 2 | 0.796 | $Fe_2O_3$. Ba |
| 3 | 0.796 | $Fe_2O_3$. S. Ba |
| 3 | 0.795 | $Fe_2O_3$. Ba. Cu |
| 4 | 0.795 | $Fe_2O_3$. S. Ba. Cu |

The whole study area was dominated by *Quinqueloculina auberiana* and *Fissurina orbignyana* (the most abundant species among the *Fissurina* genus) (Fig. 5). In the southern most station, the Miliolida order was well represented with *Q. auberiana*, *Pyrgo informata*, *Cribromiliolinella subvalvularis*, *Cruciloculina triangularis* and *Triloculina oblonga* as well as other calcareous species *Lobatula wuellerstorfi* and *Fissurina orbignyana*. Non-calcareous species (agglutinated and allogromids) were mainly present in intermediate stations (MS N; ET W and ET E) such as *Martinottiella cylindrica, Karreriella bradyi* and *Vanhoeffenella* sp. Among the most abundant species, *Gavelinopsis translucens* had its highest relative contribution in stations ET E_CL6 and SC_CL6, in the latter associated with *Epistominella exigua* and *Cibicides pachyderma*. Most common species are illustrated in plates (Figure 6). Stations Cap_CL6 and Cap_CL7 were characterized by a strong dominance of *Fissurina* spp,

(>50%) including all identified species from this genus (*F. orbignyana*, *F. annectens*, *F. foliformis*, *F. laevigata*).

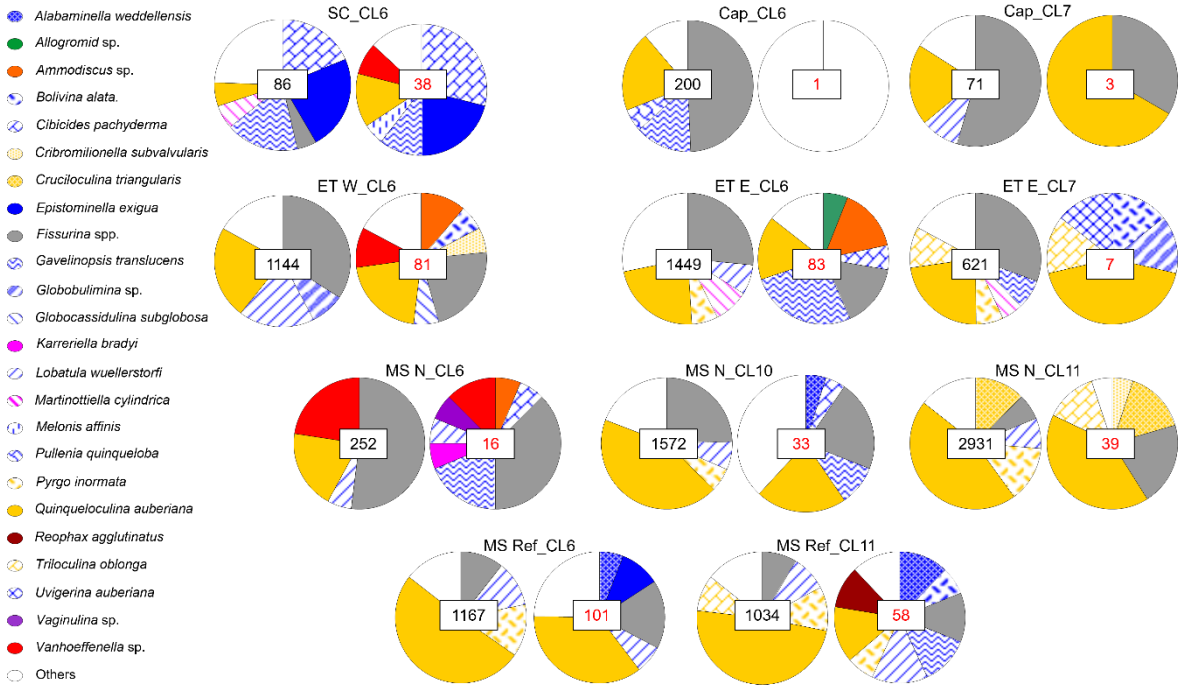


Fig. 5. Relative abundance (pie charts) and absolute number of individuals of the main benthic foraminiferal species (e.g., representing >5%) of the total abundance with dead communities represented on the left (black numbers) and living communities on the right (red numbers). Note that all *Rotalida* species are in blue and all *Miliolida* species in yellow.

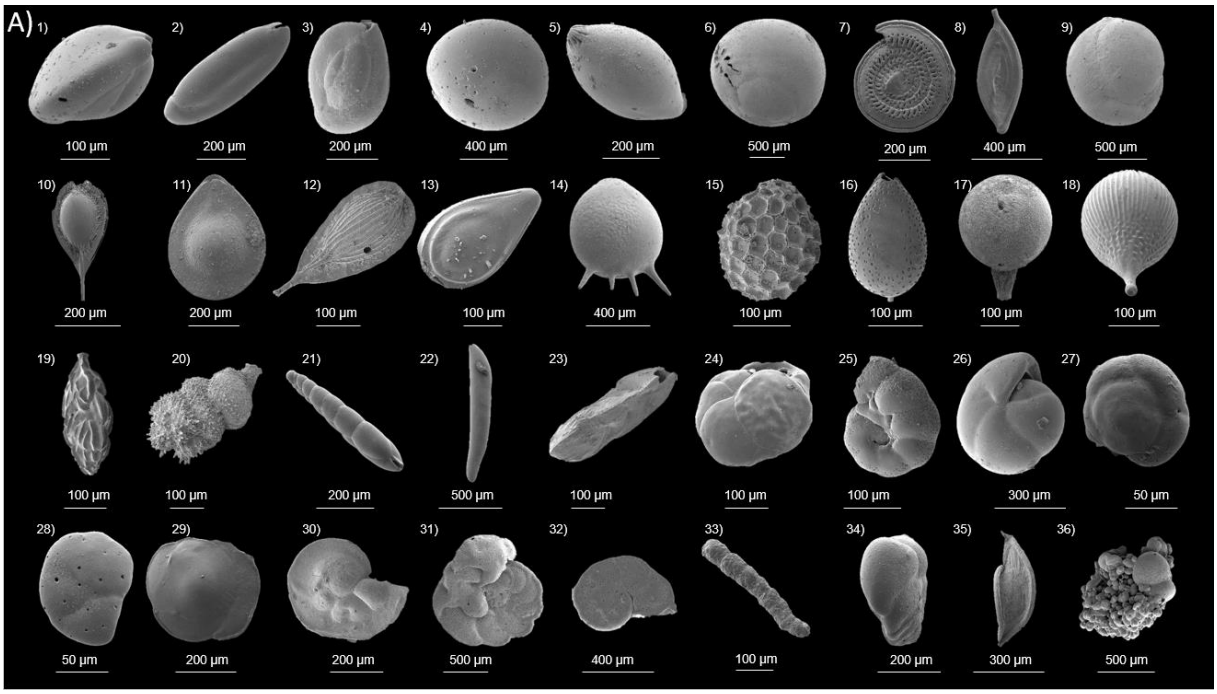



Figure 6. A) Scanning electronic microscope images of most common benthic foraminiferal species of the Lucky Strike vent field with 1) *Cruciloculina triangulis*, 2) *Triloculina oblonga*, 3) *Quinqueloculina auberiana*, 4) *Pyrgo informata*, 5) *Nevillina coronata*, 6) *Cribromiliolinella subvalvularis*, 7) *Ammodiscus* sp., 8) *Spiroloculina* sp., *9) Pyrgo depressa*, 10) *Fissurina foliformis*, 11) *Parafissurina saturni*, 12) *Fissurina striata*, 13) *Fissurina orbignyana*, 14) *Fissurina anectens*, 15) *Favulina hexagona*, 16) *Lagena laevigata*, 17) *Reussolina laevis*, 18) *Lagena striata*, 19) *Uvigerina peregrina*, 20) *Uvigerina auberiana*, 21) *Eubulimina exilis*, 22)

*Vaginulina* sp., 23) *Trifarina angulosa*, 24) *Globocassidulina subglobosa*, 25) *Melonis affinis*, 26) *Pullenia quinqueloba*, 27) *Alabaminella weddellensis*, 28) *Epistominella exigua*, 29) *Gavelinopsis translucens*, *30) Laeticarinina pauperata*, 31) *Cibicides wuellerstorfi var. lobatulus*, 32) *Cibicides wuellerstorfi*, 33) *Martinottiella cylindrica*, 34) *Karreriella bradyi*, 35) *Vanhoeffenella* sp., 36) *Reophax agglutinatus* and B) images from stereoscopic microscope of 1) *Cruciloculina triangulis*, 2) *Triloculina oblonga*, 3) *Quinqueloculina auberiana*, 4) *Pyrgo informata*, *5) Cribromiliolinella subvalvularis*, 6) *Ammodiscus* sp., 7) *Spiroloculina* sp., 8) *Spiroloculina* sp., 9) *Fissurina foliformis*, 10) *Parafissurina saturni*, 11) *Fissurina orbignyana*, 12) *Fissurina anectens*, 13) *Favulina hexagona*, 14) *Lagena laevigata*, 15) *Reussolina laevis*, 16) *Lagena striata*, 17) *Uvigerina peregrina*, 18) *Uvigerina auberiana*, 19) *Eubulimina exilis*, *20) Vaginulina* sp., 21) *Globocassidulina subglobosa*, 22) *Melonis affinis*, 23) *Pullenia quinqueloba*, 24) *Alabaminella weddellensis*, 25) *Epistominella exigua*, 26) *Gavelinopsis translucens*, 27) *Cibicides wuellerstorfi var. lobatulus*, 28) *Planulina ariminensis*, 29) *Martinottiella cylindrica*, 30) *Karreriella bradyi*, 31) *Vanhoeffenella* sp., 32) *Reophax agglutinatus.*

The RDA performed on the main species distribution selected only CaO and $Fe_2O_3$ ($p < 0.05$) when implementing the forward selection on environmental variables (Fig. 7).

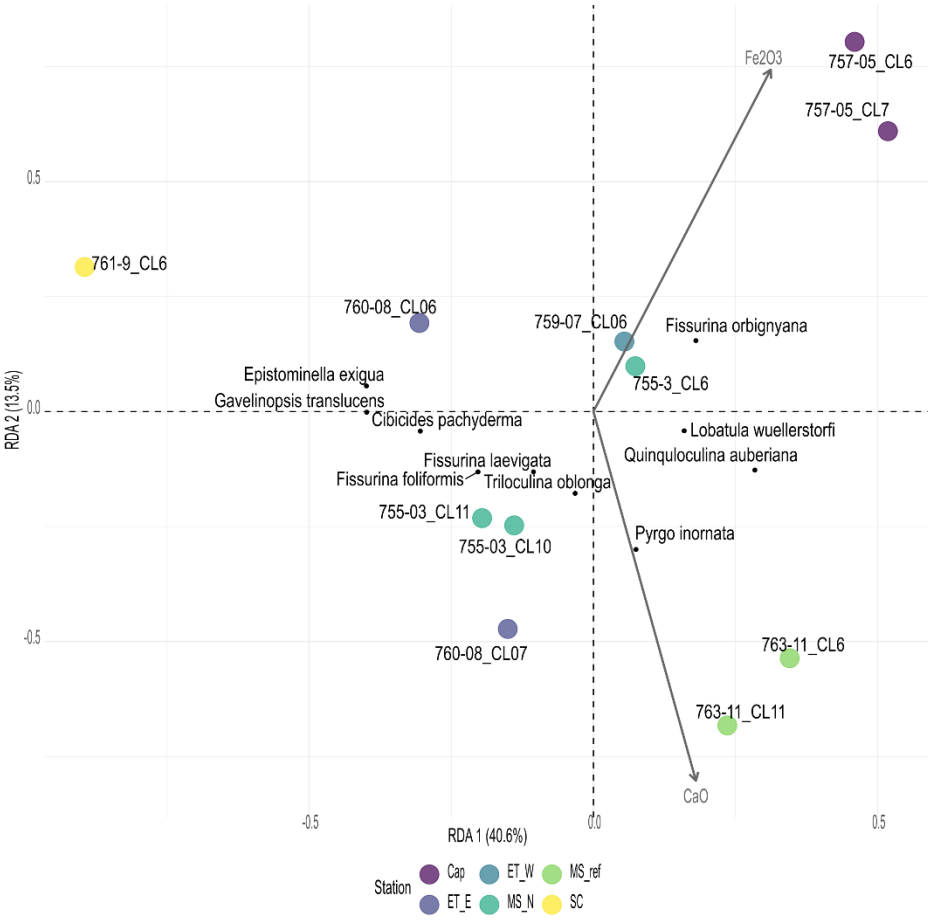

Fig. 7. Redundancy Analysis of the main benthic foraminiferal species (>5% of the total abundance) of the Lucky Strike vent field based on dead communities and environmental parameters of the top sediment layers (0-1 cm).

The RDA is significant (ANOVA-like permutation test, p = 0.007) and the first two axes represent together 54% of the data variability. Main distinctions are visible along the pelagic to hydrothermal gradient with *Q. auberiana* and *P. inornata* dominant in the reference cores on the bottom right quadrant of the RDA, associated with pelagic sedimentation (correlated to CaO) while *Fissurina orbignyana* were dominant in cores Cap_CL6 and Cap_CL7, in the most intense hydrothermal domain in the top right quadrant (correlated to $Fe_2O_3$). Cores in other venting locations are intermediate, with an exception with the South Crystal's core, showing a distinct pattern with the dominance of *E. exigua, G. translucens* and *C. pachyderma* species.

## 5. Discussion

### 5.1. Environmental control on faunal distribution

Visual observations of the habitats during the sampling showed homogenous and muddy sediment in the reference stations (MS_Ref), while larger grain size and heterogenous material characterized stations closer to the edifices. Microbial mats represented the last type of visual environments sampled, characterized by orange to brown biofilms. These three types of environments sampled were also suggested by the environmental PCA determining a pelagic domain dominated by carbonated sediments, a hydrothermal domain characterized by metal-rich sediments and microbial biofilms as benthic habitat. These habitats are controlled by the geological context, influencing the sedimentation rates, the quality and the source of the organic matter.

The Lucky Strike vent field developed on the summit of a large volcano (Ondréas et al., 2009) mainly composed of enriched mid-ocean ridge basalt (EMORB) characterized by high barium contents compared to normal MORB. This geological context allowed the enrichment in Fe and $H_2S$ in the area as well as Cu, S, Zn and Ba in the close vicinity of the black smokers (Cotte et al., 2020). Our results confirm a sedimentary content enriched in these elements at close periphery of active edifices, while further periphery mainly represents phytodetritic influence. The contribution of hydrothermal-derived material close to Eiffel Tower edifice (ET E_CL7, supplementary 4) hence represents about 2.0 cm $kyr^{-1}$ that corresponds to half of the sediment material. The elements measured in Capelinhos and South Crystal suggest an important geochemical maturation originating from the hydrothermally-derived metalliferous sediments, or more likely in Capelinhos from vestiges of inactive chimneys covering the sediment, as suggested by the pore water dissolved metals profiles (supplementary 3) thus implying a different potential impact on faunal distribution.

Inorganic carbon data appeared correlated with CaO content, mainly derived from the presence of planktonic foraminifera that were the most abundant in MS Ref stations according to visual stereoscopic microscope observations. Stable isotopic signature of the organic carbon in these stations (Table 2) demonstrated a classical marine signal of phytodetritic material (Meyers, 1994). More depleted $\delta^{13}C$ of the sedimentary organic carbon measured in the vicinity of hydrothermal edifices Eiffel Tower, Capelinhos and South Crystal and within microbial mats suggested a microbial $^{13}C$ depletion. Hence, the potential benthic foraminiferal food source varied from exclusive phytodetritic material in the MS Ref stations to mixed pelagic and microbial carbon sources in periphery stations, and exclusive microbial source in mats.

Even though statistical tests on environmental control on fauna indicate a first variance explanation based on sedimentary content (i.e., Fe, Ba and CaO), these parameters showed significant autocorrelations with TOC and $\delta^{13}C$ of the organic carbon, suggesting that

hydrothermal-derived material is strongly linked with the quantity and source of organic matter available for foraminiferal communities and should be considered for faunal interpretation. Additionally, microbial biofilms were not included in statistical tests because of the absence of fauna, being nevertheless key for distribution understanding, since they represent a significant surface covering hydrothermal vent sediments but preventing its occurrence.

### 5.2. A toxic microbial biofilm for foraminifera?

The abundance of both living and fossil benthic foraminifera suggested a main control by organic carbon content in the sediment that was not directly connected to the influence of venting activity. In particular, the cores collected on the zetaproteobacteria microbial mats (MS_CL11, MS_CL6 and ET W_CL11) revealed the absence of foraminifera. The visual observations of sediment samples pointed out the absence of all carbonated material, such as planktonic foraminifera, resulting in a very low total carbon and carbonate content (Table 2). These stalk-forming iron-oxidizing bacteria are known to produce flocculent iron oxide mats, which can be meters thick and cover hundreds of square meters (Emerson and Moyer, 2002). While oxidizing iron, they use Fe(II) and oxygen producing Fe(III) (eq. 1), that also occurs through abiotic reaction that almost directly results in the production of iron oxyhydroxides at circumneutral pH through the reaction (eq. 2) (Emerson et al., 2010).

(1) $Fe^{2+} + 0.25\ O_2 + H^+ \rightarrow Fe^{3+} + 0.5\ H_2O$

(2) $Fe^{2+} + 0.25\ O_2 + 2.5\ H_2O \rightarrow Fe(OH)_3 + 2\ H^+$

In order to limit the precipitation of Fe(III); as well as produced by the abiotic iron oxidation in iron oxyhydroxides; they excrete acidic polysaccharids that acidify (to pH = 6) their microhabitat outside their cells in order to bind the Fe(III) and prevent its precipitation in minerals (Cohen, 2020). Hence, zetaproteobacteria biofilms may significantly decrease the microenvironmental pH in their mats, resulting in the dissolution of fossil planktonic

foraminifera and preventing benthic foraminiferal colonization in surrounding sediments. These microbial communities are abundant on basaltic-rich substrates at the Lucky Strike vent field where they use the structural Fe(II) from the basaltic glass (Henri et al., 2016). Whether the absence of benthic foraminifera is explained by the presence of the microbial mats themselves (competition or lack of sediment substratum) or by the pH of the biofilm is unclear. However, the absence of all carbonated tests (planktonic foraminifera, ostracods, bivalves, gastropods) in these cores, combined with a very low inorganic carbon content in the three "microbial mat" cores further support the hypothesis of a dissolution of all carbonates in the mat. The organic carbon source there, might be limited to the microbial community itself, without pelagic contribution. Considering the sedimentation rate (2.3 cm $kyr.^{-1}$) and the carbonate content in the pelagic end-member, this dissolution would result in a rate of 0.5 $mg(CaCO_3).cm^{-3}.yr^{-1}$, that might have a significant impact on regional carbon budget considering the area covered by these mats.

### 5.3. The pelagic end-member

In the control stations (MS Ref), the organic carbon content showed its higher values in the study area, though it remained low compared to classical deep-sea environments (e.g., Dessandier et al., 2016; 2019; Krüger et al., 2025). Notably, these stations were characterized by the most abundant and diverse communities of both fossil and living benthic foraminifera. The presence of miliolid species and *L. wuellerstorfi*, characterizing these stations, suggests low inputs of organic matter derived from phytodetritic deposits, as usually observed as controlling factor for these species in the deep sea (e.g., Mackensen et al., 1995; Murgese and De Deckker, 2005; Gooday et al., 2008). The main difference in the assemblages of benthic foraminifera between the reference and intermediate stations corresponds to the decrease of miliolid relative abundance with increasing proximity to the vents. This may be explained by the calcification strategy of this order that precipitate a shell with high Mg/Ca carbonate, hence

438 necessitating an elevated pH in comparison with that of the surrounding water (de Nooijer et
439 al., 2009). Since the pH in sediments and water at Lucky Strike drastically decreases from the
440 periphery to the edifices (Sarradin et al., 1999), the energetic effort to precipitate these shells
441 may be limiting. These results are in contradiction with a recent study conducted at the Rainbow
442 vent field (Krüger et al., 2025) where miliolids have been observed in the closest relationship
443 with hydrothermal plume. This could be explained by both a different geochemical context in
444 Rainbow vent field and a different sampling strategy, with cores collected between 200 m and
445 41 km of distance to vents in Krüger et al. (2025) while all cores were distant from less than 50
446 m to chimneys in the present study (except for MS_Ref stations). Hence the closest
447 foraminiferal community to the vents in Krüger et al. (2025) is further from active chimneys
448 than all stations considered in the present study. Some *L. wuellerstorfi* individuals observed in
449 the present study morphologically resembles *Lobatula lobatula* taxon, conforming the shape of
450 their test to the substrate where they are attached. Recently, it has been demonstrated that
451 genetically identified *L. wuellerstorfi* flourishing on hard substrata present different
452 morphologies from "classical" *L. wuellerstorfi* to ecophenotype *L. wuellerstorfi* var. *lobatulus*
453 (Burkett et al., 2020). These authors proposed that both the substratum and microbial
454 colonization influence the distribution of *Cibicidae*. *Cibicides pachyderma* is a facultative
455 epifaunal species that preferentially lives as an infaunal dweller in moderate carbon flux areas,
456 able to cover parts of its test by aggregates or algae in low pH environments (Wollenburg et al.,
457 2018) where tests dissolution occurs to many deep-sea species (Corliss and Honio, 1981;
458 Murray and Alve, 1999; Pettit et al., 2013). Hence, this species may replace *L. wuellerstorfi* in
459 environments characterized by harsher environmental conditions, such as slightly lower pH or
460 because of a higher organic carbon flux due to the presence of microbes.

461 5.4. Intermediate habitats, a pool of diversity

462 The stations in the vicinity of hydrothermal edifices Eiffel Tower and Montsegur harbored
463 abundant and diverse fossil fauna while the living community remained less developed.
464 Interestingly, the faunal diversity of the living community around Eiffel Tower appeared
465 relatively high, showing abundant non-calcareous species (e.g., *Vanhoeffenela* sp., *Reophax*
466 *agglutinatus*, *Martinotiella cylindrica* and allogromid sp.) and *Globocassidulina subglobosa*
467 that were rare in the rest of the stations. Monothalamids may be present in a greater extent due
468 to harder substrata where they can attach their test, preferentially to most of the calcareous taxa.
469 Their occurrence at Lucky Strike was however limited, in comparison with other deep-sea
470 environments (e.g., Koho et al., 2007) potentially because of low pH microenvironments. As
471 observed for agglutinated species in cold seeps (e.g., Heinz et al., 2005; Panieri and Sen Gupta,
472 2008; Martin et al., 2010, Dessandier et al., 2019), these species might not easily tolerate the
473 environmental conditions derived from hydrothermal venting. Nevertheless, several
474 agglutinated species represent pioneer recolonizers following the end of venting or sediment
475 disturbance (Kitazato, 1995; Panieri et al., 2005) and may flourish on inactive chimneys. The
476 cores collected in sediments enriched in iron and sulfur (Capelinhos) displayed generally lower
477 dead faunal abundances than those from the intermediate stations due to very low living fauna.
478 Interestingly, South Crystal site, that is more a mix of basalt and metalliferous sediment, is
479 characterized by a substantial living individuals' density and a slightly different faunal
480 distribution, with *G. translucens*, *E. exigua* and *C. pachyderma* as the most abundant species.
481 This assemblage highlights a potential fresher organic material than in the other stations that
482 may be linked to a higher microbial productivity, triggered by the high content in iron and
483 sulfur. Sen Gupta and Aharon (1994) observed *G. translucens* as a dominant taxon in a bathyal
484 vent community of the Gulf of Mexico, associated with bacterial (*Beggiatoa*) mats and tolerant
485 to anoxic conditions and high $H_2S$ concentrations in sediments. Many opportunistic deep-sea
486 species may experience dormancy phases during periods of starvation and are likely able to

switch to a biologically active phase when phytodetritus pulses reach the seafloor (Gooday and Rathburn, 1999), with a response that differs at daily to seasonal scales. In bathyal north Atlantic environment, *Quinqueloculina* sp. has been observed as dominant in late summer, after the degradation of fresh phytodetritic material, replacing opportunistic species (e.g., *Alabaminella weddellensis*, *E. exigua*) at the sediment water interface, after a probable migration up from a shallow infaunal microhabitat (Gooday and Rathburn, 1999). This phenomenon could explain the dominance of *Q. auberiana* in our study area sampled in September while opportunistic species (*G. translucens* and *E. exigua* and *A. weddellensis*) are restricted to sediments harboring additional food sources represented by microbial communities. *Epistominella exigua* and *A. weddellensis* represent the most common species in the deep-sea Atlantic Ocean in the >63 µm size fraction (Sun et al., 2006) as in the present study in intermediate stations. These opportunistic species flourish whenever suitable food sources - such as phytoplankton or microorganisms (Turley et al., 1993)- become available (Gooday, 1988).

### 5.5. Capelinhos, the sulfide-rich metalliferous microhabitat

The foraminiferal living community was absent in Capelinhos where the very high content in hydrothermal-derived elements have probably directly or indirectly restrained foraminiferal growth. However, considering the elevated number of fossils in these two stations, it is clear that the microenvironment is not preventing colonization by benthic foraminifera as observed in the zetaproteobacterial mats. An equilibrium between the source of energy that promotes microbial communities and the more classical marine conditions represented in the reference stations seems to be necessary for the development of these opportunistic species that can thrive in sediments slightly impacted by venting. Surprisingly, a strong fossil dominance of *Fissurina orbignyana* has been observed in the two Capelinhos stations as well as in one of the intermediate stations around Montsegur edifice. Very little is known about the ecology of the

genus *Fissurina*, often observed in deep-sea environments, but never abundant enough to decipher its ecology. Its occurrence in both the intermediate and extreme environments (i.e., rich in Fe, S and Cu) suggest a wide range of tolerance for these single chambered specimens, which would necessitate further investigations allowing to find more living individuals to determine their single ecology. Even though Capelinhos edifice lies in a different chemical domain than other edifices of the Lucky Strike vent field (Chavagnac et al. 2018), with the most enriched metal content (Cotte et al., 2020), we cannot exclude that the fossils observed of *Fissurina* species come from a period of a less intense vent activity. Alternatively, the more intense hydrothermal impact observed in this particular core may reflect a different source of particles that could originate from dismantled past chimneys, hence representing harsher environment than diffusion of metal from particles deposited through the hydrothermal plume. Further investigations on the tolerance of these species for high metallic content may be of interest in the future to better understand the ecology of this group.

## 6. Conclusions

Extensive symbiotic relationships between microorganisms and macrofauna, as well as too limited number of studies on vent meiofauna, lead to a bypass of meiofauna as major contributors in the vent trophic network. This limited role in energy transfer may explain why meiofauna -especially foraminifera- has received relatively little attention in these ecosystems. However, benthic foraminifera represent an essential chain of the deep-sea food web, making a link between phytoplanktonic and microbial communities on which they feed and a substantial number of predators from the metazoans feeding on foraminifera. In hydrothermal systems, the environmental conditions represent a challenge for these organisms to thrive (e.g., low pH, high $H_2S$ content, hard substrates and in particular low organic carbon content), hence leading to a

crucial role of microbial communities as an additional food source but also by the role they have in changing the environment (e.g., consuming $H_2S$).

Our results demonstrated that the microbial food source allowed benthic foraminiferal opportunistic species to flourish in the direct vicinity to active chimneys where the elements present in the sediment (Fe, S) originated high microbial content. In the reference cores, the foraminiferal community showed adaptation for more refractory organic matter, which is partially explained by the period of sampling. Directly opposed to this trend, the establishment of biofilm from Zetaproteobacteria seems to trigger the dissolution of all carbonated shells. A direct *in situ* pH measurement would confirm this hypothesis hence representing a key perspective of this work. The absence of agglutinated or organic-walled specimens in these mats even revealed a toxic environment for all benthic foraminifera. This observation questions the role of these extended microbial mats in the carbon fluxes in hydrothermal vent systems, with the dissolution of foraminiferal tests that might export carbon from the sediment to the water column. The reasons for the establishment of mats of Zetaproteobacteria remains uncertain (Emerson et al., 2010), and no direct link can be made when focusing on the iron content in the sediment. This observation points out the extreme heterogeneity of the hydrothermal-derived microhabitats that affects the regional biodiversity where benthic foraminifera represent a powerful bio-indicator.

In the absence of symbiosis between microbes and macrofauna that occurs only in active hydrothermal vents, benthic foraminifera may represent a key element of the trophic chain for the inactive systems. In metalliferous sediments as the intermediate stations studied here, benthic foraminiferal communities showed their highest diversities. These environments represent good analogues for inactive hydrothermal chimneys inhabited by microbial communities that use reduced elements accumulated in the sediments. These systems are nowadays under the scope of the society for economic interests in metalliferous sediment

associated to sulfides deposits and consequently threaten. Hence, the local high diversity observed would be clearly impacted by removal the life conditions of benthic foraminifera. Therefore, a good knowledge on benthic foraminiferal ecology from these environments, close to active vents, in the periphery and on inactive chimneys appears essential to prevent any damage in the deep-sea biodiversity. Further analyses, especially regarding the trophic networks would greatly improve this knowledge in the future.

## Acknowledgements

The authors would like to thank the captain and the crew of the *R/V Pourquoi Pas?* and the chief scientist P.M. Sarradin. This work was supported by ISblue project, Interdisciplinary graduate school for the blue planet (ANR-17-EURE-0015) and co-funded by a grant from the French government under the program "Investissements d'Avenir", and by a grant from the Regional Council of Brittany (SAD programme). We thank J.H. Ogor, M. Hubert, Y. Germain and N. Gayet for their technical help in data acquisition.

## References

Alfaro-Lucas, J.M., Pradillon, F., Zeppilli, D., Michel, L.N., Martinez-Arbizu, P., Tanaka, H., Foviaux, M., Sarrazin, J., 2020. High environmental stress and productivity increase functional diversity along a deep-sea hydrothermal vent gradient. Ecology 101(11), e031144.

Alongi, D. M., & Pichon, M., 1988. Bathyal meiobenthos of the western Coral Sea: distribution and abundance in relation to microbial standing stocks and environmental factors. Deep Sea Research Part A. Oceanographic Research Papers, 35(4), 491-503.

Altenbach, A. V., Pflaumann, U., Schiebel, R., Thies, A., Timm, S., & Trauth, M., 1999. Scaling percentages and distributional patterns of benthic foraminifera with flux rates of organic carbon. The Journal of Foraminiferal Research, 29(3), 173-185.

586 Astorch-Cardona, A., Odin, G. P., Chavagnac, V., Dolla, A., Gaussier, H., & Rommevaux, C.,
587 2024. Linking Zetaproteobacterial diversity and substratum type in iron-rich microbial mats
588 from the Lucky Strike hydrothermal field (EMSO-Azores observatory). Applied and
589 Environmental Microbiology, 90(2), e02041-23.

590 Bernhard, J. M., & Panieri, G., 2018. Keystone Arctic paleoceanographic proxy association
591 with putative methanotrophic bacteria. Scientific Reports, 8(1), 10610.

592 Burkett, A.M., Rathburn, A., Elena Pérez, M., Martin, J.B., 2018. Influences of thermal and
593 fluid characteristics of methane and hydrothermal seeps on the stable oxygen isotopes of living
594 benthic foraminifera. Marine and Petroleum Geology 93, 344-355.

595 Burkett, A., Rathburn, A., Pratt, R.B., Holzmann, M., 2020. Insights into the ecology of
596 epibenthic calcareous foraminifera from a colonization study at 4000 m (Station M) in the NE
597 Pacific Ocean. Deep Sea Research II: Topical Studies in Oceanography 173, 104709.

598 Childress, J.J., and Fisher, C.R., 1992. The biology of hydrothermal vent animals: physiology,
599 bio-chemistry and autotrophic symbioses. Oceanography and Marine Biology 30:337–441

600 Cohen, 2020. The Ecophysiology of Iron-Oxidizing Zetaproteobacteria: Microbe-Mineral
601 Interactions, Transcriptomic Responses, and Biomineralization. PhD Thesis

602 Cotte, L., Chavagnac, V., Pelleter, E., Laës-Huon, A., Cathalot, C., Dulaquais, G., Riso, R.D.,
603 Sarradin, P.-M., Waeles, M., 2020. Metal partitioning after in situ filtration at deep-sea vents
604 of the Lucky Strike hydrothermal field (EMSO-Azores, Mid-Atlantic Ridge, 37°N). Deep Sea
605 Research I: Oceanographic Research Papers 157, 103204.

606 de Nooijer, L., Toyofuku, T., Kitazato, H., 2009. Foraminifera promote calcification by
607 elevating their intracellular pH. Proceedings of the National Academy of Sciences of the United
608 States of America 106 (36), 15374-15378.

609 Desbruyeres, D., Biscoito, M., Caprais, J.-C., Colaço, A., Comtet, T., Crassous, P., Fouquet,
610 Y., Khripounoff, A., Le Bris, N., Olu, K., Riso, R., Sarradin, P.-M., Vangriesheim, A., 2001.
611 Variations in deep-sea hydrothermal vent communities on the Mid-Atlantic Ridge near the
612 Azores plateau. Deep Sea Research I: Oceanographic Research Papers 48 (5), 1325-1346.

613 Dessandier, P.-A., Bonnin, J., Kim, J.-H., Bichon, S., Deflandre, B., Grémare, A., Sinninghe
614 Damsté, J.S., 2016. Impact of organic matter source and quality on living benthic foraminiferal

615 distribution on a river-dominated continental margin: a study of the Portuguese margin. Journal
616 of Geophysical Research, Biogeosciences 121, 1689–1714.

617 Dessandier, P.-A., Borrelli, C., Kalenitchenko, D., Panieri, G., 2019. Benthic foraminifera in
618 Arctic methane hydrate bearing sediments. Frontier in Marine Science 6:765.
619 https://doi.org/10.3389/fmars.2019.00765

620 Emerson, D., and Moyer, C.L., 2002. Neutrophilic Fe-Oxidizing Bacteria Are Abundant at the
621 Loihi Seamount Hydrothermal Vents and Play a Major Role in Fe Oxide Deposition. Applied
622 and Environmental Microbiology 68 (6), 3085-3093.

623 Fisher, C., Takai, K., Le Bris, N., 2007. Hydrothermal vent ecosystems. Oceanography 20: 14-
624 23

625 Fouquet, Y., Ondréas, H., Charlou, J.-L., Donval, J.-P., Radford-Knoery, J., Costa, I., Lourenço,
626 N., Tivey, M.K., 1995. Atlantic lava lakes and hot vents. Nature 377, 201.

627 Gooday, A.J., 1988. A response by benthic foraminifera to phytodetritus deposition in the deep
628 sea. Nature 332, 70–73

629 Gooday, A.J., 1994. The biology of deep-sea foraminifera: A review of some advances and
630 their applications in paleoceanography. Palaios 9, 14-31.

631 Gooday, A.J., and Rathburn, A., 1999. Temporal variability in living deep-sea benthic
632 foraminifera: a review. Earth-Science Reviews 46 (1-4), 187-212.

633 Gooday, A. J., Nomaki, N. H., & Kitazato, H., 2008. Modern deep-sea benthic foraminifera: a
634 brief review of their morphology-based biodiversity and trophic diversity.

635 Heinz, P., Sommer, S., Pfannkuche, O., Hemleben, C., 2005. Living benthic foraminifera in
636 sediments influenced by gas hydrates at the Cascadia convergent margin, NE Pacific. Mar.
637 Ecol. Prog. Ser.30477–89. 10.3354/meps304077

638 Henri, P.A., Rommevaux-Jestin, C., Lesongeur, F., Mumford, A., Emerson, D., Godfroy, A.,
639 Ménez, B., 2016. Structural Iron (II) of Basaltic Glass as an Energy Source for
640 Zetaproteobacteria in an Abyssal Plain Environment, Off the Mid Atlantic Ridge. Frontiers in
641 Microbiology. https://doi.org/10.3389/fmicb.2015.01518

642 Hollander D.J., Smith M.A., 2001. Microbially mediated carbon cycling as a control on the
643 d13C of sedimentary carbon in eutrophic Lake Mendota (USA): new models for interpreting
644 isotopic excursions in the sedimentary record. Geochim Cosmochim Acta 65, 4321-4377.

Husson, B., Sarradin, P.M., Zeppilli, D., Sarrazin, J., 2017. Picturing thermal niches and biomass of hydrothermal vent species. Deep-Sea Res. II Top. Stud. Oceanogr. 137, 6–25. https://doi.org/10.1016/j.dsr2.2016.05.028.

Jonasson, K.E., Schröder-Adams, C.J., Patterson, R.T., 1995. Benthic foraminiferal distribution at Middle Valley, Juan de Fuca Ridge, a northeast Pacific hydrothermal venting site. Marine Micropaleontology 25 (2-3), 151-167.

Jorissen, F.J., de Stigter, H.C., Widmark, J.G., 1995. A conceptual model explaining benthic foraminiferal microhabitats. Marine Micropaleontology 26, 3–15.

Khripounoff, A., Comtet, T., Vangriesheim, A., Crassous, P., 2000. Near-bottom biological and mineral particle flux in the Lucky Strike hydrothermal vent area (Mid-Atlantic Ridge). Journal of Marine Systems 25 (2), 101-118.

Kitazato, H., 1995. Recolonization by deep-sea benthic foraminifera: possible substrate preferences. Marine Micropaleontology 26 (1-4), 65-74.

Koho, K.A., Kouwenhoven, T.J., de Stigter, H.C., van der Zwaan, G.J., 2007. Benthic foraminifera in the Nazaré Canyon, Portuguese continental margin: Sedimentary environments and disturbance. Marine Micropaleontology 66, 27-51.

Krüger, H., Schmiedl, G., Steiner, Z., Zhang, Z., Achterberg, E. P., & Glock, N., 2025. Change in biodiversity and abundance of benthic foraminifera with distance from the Rainbow hydrothermal vent field, Mid-Atlantic Ridge. Journal of Micropalaeontology, 44(2), 193-211.

Kurt, R. B., & Barry, J. B., 1998. Monterey Bay cold seep infauna: quantitative comparison of bacterial mat meiofauna with non-seep control sites. Cahiers Biol. Mar, 39, 333-335.

Langmuir, C., Humphris, S., Fornari, D., Van Dover, C., Von Damn, K., Tivey, M.K., Colodner, D., Charlou, J.-L., Desonie, D., Wilson, C., Fouquet, Y., Klinkhammer, G., Bougault, H., 1997. Hydrothermal vents near a mantle hot spot: the Lucky Strike vent field at 37°N on the Mid-Atlantic Ridge. Earth and Planetary Science Letters 148 (1-2), 69-91.

Levin, L. A., & Gooday, A. J., 2003. The deep atlantic ocean. Ecosystems of the World, 111-178.

Loeblich Jr, A. R., & Tappan, H., 1987. Foraminiferal evolution, diversification, and extinction. Journal of Paleontology, 695-714.

Loubere, P., & Fariduddin, M., 1999. Benthic foraminifera and the flux of organic carbon to the seabed. Modern foraminifera, 181-199.

Mackensen, A., Schmiedl, G., Harloff, J., & Giese, M., 1995. Deep-sea foraminifera in the South Atlantic Ocean: ecology and assemblage generation. Micropaleontology, 342-358.

Martin, R. A., Nesbitt, E. A., Campbell, K. A., 2010. The effects of anaerobic methane oxidation on benthic foraminiferal assemblages and stable isotopes on the Hikurangi Margin of eastern New Zealand.Mar. Geol.272270–284. 10.1016/j.margeo.2009.03.024

Matabos, M., Cannat, M., Ballu, V., Barreyre, T., Blandin, J., Castillo, A., ... & Sarradin, P. M., 2025. The EMSO-Azores deep-sea observatory: 15 years of multidisciplinary studies of the lucky strike hydrothermal system, from sub-seafloor to the water column. Journal of Sea Research, 102625.

Meyers, P.A., 1994. Preservation of elemental and isotopic source identification of sedimentary organic matter. Chemical Geology 114, 289-302.

Molina-Cruz, A., and Ayala-Lopez, A., 1988. Influence of the hydrothermal vents on the distribution of benthic foraminifera from the Guaymas Basin, Mexico. Geo-Marine Letters 8, 49-56.

Murgese, D. S., & De Deckker, P., 2005. The distribution of deep-sea benthic foraminifera in core tops from the eastern Indian Ocean. Marine Micropaleontology, 56(1-2), 25-49.

Murray, J. W., & Alve, E., 1999. Natural dissolution of modern shallow water benthic foraminifera: taphonomic effects on the palaeoecological record. Palaeogeography, Palaeoclimatology, Palaeoecology, 146(1-4), 195-209.

Oksanen, J., Simpson, G. L., Blanchet, F. G., Kindt, R., Legendre, P., Minchin, P. R., ... & Weedon, J. (2001). Vegan: community ecology package.

Ondréas, H., Cannat, M., Fouquet, Y., Normand, A., Sarradin, P.-M., Sarrazin, J., 2009. Recent volcanic events and the distribution of hydrothermal venting at the Lucky Strike hydrothermal field, Mid-Atlantic Ridge. Geochemistry, Geophysics, Geosystems 10 (2). https://doi.org/10.1029/2008GC002171

Panieri, G., 2005. Benthic foraminifera associated with a hydrocarbon seep in the Rockall Trough (NE Atlantic). Geobios 38, 247–255.

Panieri, G., 2006. Foraminiferal response to an active methane seep environment: a case study from the Adriatic Sea. Marine Micropaleontology, 61(1-3), 116-130.

Panieri, G., Sen Gupta, B. K., 2008. Benthic foraminifera of the blake ridge hydrate mound, Western North Atlantic Ocean. Mar. Micropaleontol. 6691–102. 10.1016/j.marmicro.2007.08.002

Pelleter, E., Fouquet, Y., Etoubleau, J., Cheron, S., Labanieh, S., Josso, P., Bollinger, C., Langlade, J., 2017. Ni-Cu-Co-rich hydrothermal manganese mineralization in the Wallis and Futuna back-arc environment (SW Pacific). Ore Geology Reviews 87, 126-146.

Pettit, L. R., Hart, M. B., Medina-Sánchez, A. N., Smart, C. W., Rodolfo-Metalpa, R., Hall-Spencer, J. M., & Prol-Ledesma, R. M., 2013. Benthic foraminifera show some resilience to ocean acidification in the northern Gulf of California, Mexico. Marine Pollution Bulletin, 73(2), 452-462.

R Core Team (2025). R: A language and environment for statistical computing. R Foundation for Statistical Computing, Vienna, Austria. https://www.R-project.org/.

Reimer, P.J., et al., 2013. Intcal13 and Marine13 radiocarbon age calibration curves 0-50,000 years cal bp. Radiocarbon 55 (4), 1869e1887.

Sarradin, P.-M., Caprais, J.-C., Riso, R., Kérouel, R., Aminot, A., 1999. Chemical environment of the hydrothermal mussel communities in the Lucky Strike and Menez Gwen vent fields, Mid Atlantic Ridge. Cahiers de Biologie Marine 40, 93-104

Sarradin, P.-M., M. Waeles, S. Bernagout, C. Gall, J. Sarrazin, and R. Riso. 2009. Speciation of dissolved copper within an active hydrothermal edifice on the Lucky Strike vent field (MAR, 37°N). Science of the Total Environment 407:869–878.

Sarrazin, J., P. Legendre, F. de Busserolles, M.-C. Fabri, K. Guilini, V. N. Ivanenko, M. Morineaux, A. Vanreusel, and P.-M. Sarradin. 2015. Biodiversity patterns, environmental drivers and indicator species on a high-temperature hydrothermal edifice, Mid-Atlantic Ridge. Deep Sea Research Part II: Topical Studies in Oceanography 121:177–192.

Sarrazin, J., Portail, M., Legrand, E., Cathalot, C., Laes, A., Lahaye, N., Husson, B., 2020. Endogenous versus exogenous factors: what matters for vent mussel communities? Deep-Sea Res. I Oceanogr. Res. Pap. 160, 103260. https://doi.org/10.1016/j. dsr.2020.103260.

Schmidt, C., Vuillemin, R., Le Gall, C., Gaill, F., & Le Bris, N., 2008. Geochemical energy sources for microbial primary production in the environment of hydrothermal vent shrimps. Marine Chemistry, 108(1-2), 18-31.

Sen Gupta, B.K., Aharon, P., 1994. Benthic foraminifera of bathyal hydrocarbon vents of the Gulf of Mexico: initial report on communities and stable isotopes. Geo-Marine Letters 14, 88–96.

Stuiver, M., Reimer, P.J., Reimer, R., 2014. CALIB radiocarbon calibration execute, version 7.0html. Available online at: http://calib.qub.ac.uk/calib/.

Sun, X., Corliss, B., Brown, C.W., Showers, W.J., 2006. The effect of primary productivity and seasonality on the distribution of deep-sea benthic foraminifera in the North Atlantic. Deep Sea Research Part I: Oceanographic Research Papers 53 (1), 28-47

Turley, C.M., Gooday, A.J., Green, J.C., 1993. Maintenance of abyssal benthic foraminifera under high pressure and low temperature: some preliminary results. Deep Sea Research Part I: Oceanographic Research Papers 40 (4), 643-652

Van Dover, C.L., 1995. Ecology of Mid-Atlantic Ridge hydrothermal vents. In: Parson, L.M., Walker, C.L., Dixon, D.R. (Eds.), Hydrothermal Vents and Processes 87. The Geological Society of London Special Publication 257–294.

Van Dover et al., 1996

Wollenburg, J.E., Zittier, Z.M., Bijma, J., 2018. Insight into deep-sea life–Cibicidoides pachyderma substrate and pH-dependent behaviour following disturbance. Deep Sea Research Part I: Oceanographic Research Papers 138, 34-45

## Conflicts of Interest

The authors declare no conflicts of interest.

## Data Availability Statement

All data have been provided as supplementary material

## Authors contribution

PAD designed the experiments, identified benthic foraminifera and analyzed the data. GP and JS supervised the project. RL contributed to statistical analyses and figures. EP, AB and SC analyzed and interpreted the geological data. AB and SF contributed to biological sampling and samples processing. All authors revised the manuscript.